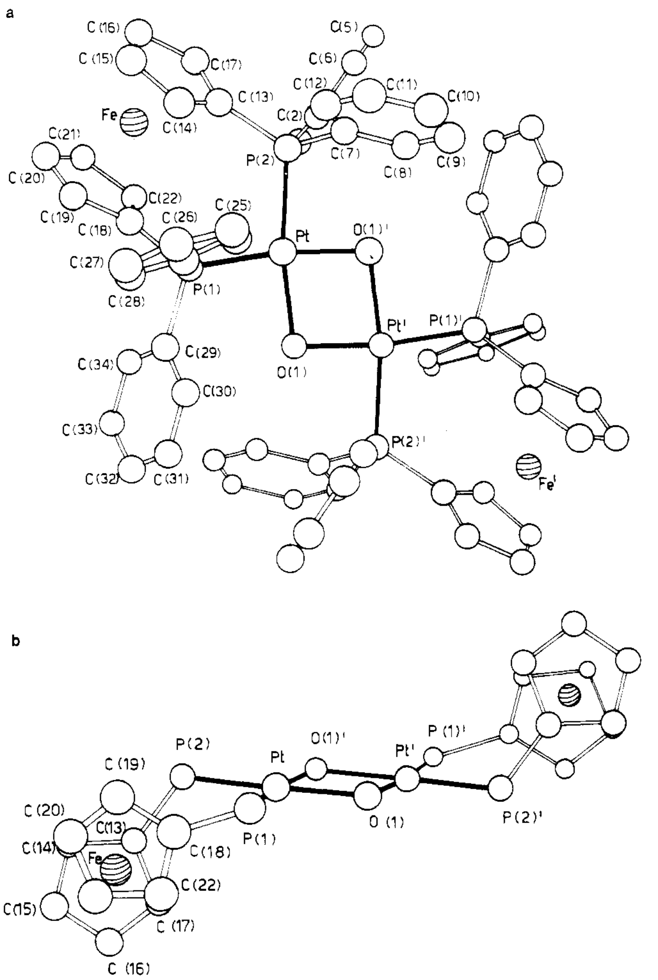

Figure 1. Views of **4**-Pt. The trapped molecules and the anionic counterions are omitted for clarity; in part b the C_6H_5 groups are also omitted. Structural parameters (see also text) are as follows: distances, Pt–P(1) = 2.230 (4), Pt–P(2) = 2.253 (4), Pt–O = 2.100 (11), Pt–Pt = 3.227 (1), Pt–Fe = 4.172 (4), C–Fe = 2.045 (av) Å; angles, Pt–O–Pt = 100.6 (7), P(1)–Pt–P(2) = 98.1 (1), P(1)–Pt–O = 92.3 (3), P(2)–Pt–O = 169.5 (4), P(2)–Pt–O′ = 90.2 (3); O–Pt–O′ = 79.4 (4)°.

ethane $[(dppe)M(\mu\text{-}Cl)]_2^{2+}$.[11] However, two major differences are to be noted: (i) the resistance to bridge splitting appears to be stronger in the dppe complexes, which maintain their dimeric nature in acetonitrile, and (ii) the solvolytic stability toward chloride displacement of the relevant parent complexes, (dppe)MCl_2, appears to be much lower in coordinating solvents (e.g. DMSO) than that observed in complexes **1**. In fact, **1**-Pt appears to be quite unreactive in this last solvent also after heating at 90 °C for 24 h.

Cyclic voltammetric (CV) experiments in 1,2-dichloroethane show that all complexes herein described undergo a reversible one-electron-transfer reaction involving the ferrocene moiety and the relevant standard potentials are significantly sensitive to the nature of the extra ligands.[12] The CV response of complexes **2** does remarkably exhibit the same shape and current values as that of the monomeric species **1**, into which they can be easily converted in situ, upon addition of the stoichiometric amount of Bu_4NCl. This is in full agreement with a complete lack of interaction between the two electroactive centers in the same molecule.[13]

Solid-State Structure of 4-Pt. The molecular structure of the cationic complex is depicted in Figure 1.

The ligand geometry around the Pt atoms is distorted square planar, as shown by the larger P–Pt–P angle (98.1 (1)°), by the smaller P(2)–Pt–O angle (169.5 (4)°), and by the distance of the Pt atoms from the two P and two O mean planes (±0.014 Å). The P(1)–Pt–P(2) angles as well as the Pt–P bond lengths are quite similar to those observed in **1**-Pt.[14] As expected, the $P_4Pt_2O_2$ skeleton is planar and this finding is in striking contrast with the lack of coplanarity observed in the only further example of an X-ray-investigated phosphino–hydroxo–platinum(II) complex, *cis*-$[(PEt_3)_2Pt(\mu\text{-}OH)]_2(BF_4)_2$.[4] In this complex, in fact, the plane normals of the PtP_2O_2 halves form an angle of 36.4°. The Pt–O distance in **4**-Pt (2.100 (11) Å) is significantly longer than that observed in the closely related, i.e. coplanar, bridged hydroxo platinum(II) complex $[(NH_3)_2Pt(\mu\text{-}OH)]_2^{2+}$ (2.03 (1) Å).[15] The Pt–O–Pt angle is also remarkably larger than in the amino complex (100.6 (7) vs 81.3 (4)°), so that also the Pt–Pt distance turns out to be considerably greater (3.227 (1) vs 3.085 (1)°). The Fe atoms are displaced 1.69 Å from the Pt_2O_2 plane, and the two cyclopentadienyl rings, which do not deviate significantly from planarity, are in the staggered configuration and form an angle equal to 5.0°. Similar to what is observed for **1**-Pt,[14] the ring spacing decreases toward the phosphorus atoms.

Water and dichloromethane molecules as well as the BF_4^- ions do not chemically interact with the cationic complex (Pt–Cl distance 3.824 (5) Å and Pt–O distance ≥4 Å). Water molecules are hydrogen-bonded to BF_4^- (O–F = 3.012 (30) Å), while the dichloromethanes are simply trapped inside the crystal lattice.

Single crystals of **4**-Pd were also obtained, and the preliminary X-ray data show that it is isotypic and therefore isostructural with **4**-Pt.

Acknowledgment. We are grateful to Prof. B. Lippert for helpful discussion.

Registry No. 1 (M = Pd), 72287-26-4; **1** (M = Pt), 104413-90-3; **2** (M = Pd), 112220-68-5; **2** (M = Pt), 106354-45-4; **4** (M = Pd), 112220-70-9; **4** (M = Pt), 112220-72-1; **5** (M = Pt), 112295-40-6.

Supplementary Material Available: Listings of selected bond distances and angles, thermal parameters, and mean planes equations (4 pages); a complete listing of structural data (including *F*) (18 pages). Ordering information is given on any current masthead page.

---

(11) (a) Davies, J. A.; Hartley, F. R.; Murray, S. G. *J. Chem. Soc., Dalton Trans.* **1979**, 1705. (b) Davies, J. A.; Hartley, F. R.; Murray, S. G. *Inorg. Chem.* **1980**, *19*, 2299.

(12) Standard potentials for two-step charge transfers obtained by comparison of experimental cyclic voltammetry data to the theoretical parameters in Table II of ref 13: **2**-Pd, $E°_1$ = 0.718 V, $E°_2$ = 0.754 V; **2**-Pt, $E°_1$ = 0.707 V, $E°_2$ = 0.743 V; **4**-Pd, $E°_1$ = 0.662 V, $E°_2$ = 0.698 V; **4**-Pt, $E°_1$ = 0.650 V, $E°_2$ = 0.686 V.

(13) Richardson, D. E.; Taube, H. *Inorg. Chem.* **1981**, *20*, 1278.

(14) Clemente, D. A.; Pilloni, G.; Corain, B.; Longato, B.; Tiripicchio-Camellini, M. *Inorg. Chim. Acta* **1986**, *115*, L9.

(15) Faggiani, R.; Lippert, B.; Lock, C. J. L.; Rosenberg, B. *J. Am. Chem. Soc.* **1977**, *99*, 777.

Contribution from the Department of Chemistry,
University of Massachusetts, Amherst, Massachusetts 01003

Mononuclear and Tetranuclear Diorganotin(IV) Carboxylates from the Reaction of Dimethyltin Oxide with Anthranilic Acid and Its *p*-Amino Isomer

V. Chandrasekhar, Roberta O. Day, Joan M. Holmes,
and Robert R. Holmes*

Received August 26, 1987

Hydrolysis of diorganotin compounds, R_2SnX_2, results in the formation of organostannoxanes.[1-5] Although initially this class of compounds was thought to be monomeric,[6] subsequent work

---

(1) Pentacoordinated Molecules. 72. Part 71: Holmes, R. R.; Shafieezad, S.; Chandrasekhar, V.; Holmes, J. M.; Day, R. O. *J. Am. Chem. Soc.* **1988**, *110*, 1174.

(2) (a) Okawara, R.; Wada, M. *J. Organomet. Chem.* **1963**, *1*, 81. (b) Alleston, D. L.; Davies, A. G.; Hancock, M. *J. Chem. Soc.* **1964**, 5744.

(3) Harada, T. *Sci. Pap. Inst. Phys. Chem. Res.* (*Jpn.*) **1939**, *35*, 290.

(4) Okawara, R.; Wada, M. *Adv. Organomet. Chem.* **1967**, *5*, 137-167 and references cited therein.

(5) Vollano, J. F.; Day, R. O.; Holmes, R. R. *Organometallics* **1984**, *3*, 745.

in solution and in the solid state demonstrated the oligomeric nature of these compounds.[5,7-13] X-ray structures of $[Me_2ClSnOSnMe_2Cl]_2$, $[Et_2ClSnOSnMe_2Cl]_2$,[8] $[i\text{-}Pr_2ClSnOSnMe_2Cl\text{-}i\text{-}Pr]_2$,[9] $[Me_2(NCS)Sn{-}O{-}Sn(NCS)Me_2]_2$,[10] $[Me_2Sn(OSiMe_3)OSn(OSiMe_3)Me_2]_2$,[11,12] $[(i\text{-}Pr)_2ClSn{-}O{-}Sn(i\text{-}Pr)_2OH]_2$,[13] $[(Me_3SiCH_2)_2ClSn{-}O{-}Sn(Me_3SiCH_2)_2OH]_2$,[13] $[(Me_3SiCH_2)_2(OH)Sn{-}O{-}Sn(Me_3SiCH_2)_2OH]_2$,[9] and more recently $[Ph_2SnCl{-}O{-}SnClPh_2]_2$ and $[Ph_2SnCl{-}O{-}Sn(OH)Ph_2]_2$,[5] reveal that all of these compounds possess a planar "ladder" type of structure containing dimeric distannoxane units with tin atoms in a trigonal-bipyramidal framework.

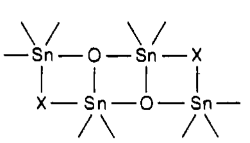

However, the trimethylsiloxy derivative $[Me_4Sn_2(OSiMe_3)_2O]_2$[11,12] is described more accurately as a "staircase". In solution two signals are observed for the chemically different tin atoms in the ^{119}Sn NMR, indicating retention of the solid-state structures.

Recently, Sandhu et al.[14] have reported analogous formulations, $R_2LSnOSnLR_2$, where L = *N*-acetyl-L-leucine or *N*-acetyl-L-phenylalanine, obtained from the reaction of dialkyltin oxides and *N*-acetylamino acids. On the basis of IR and ^{119}Sn Mössbauer spectroscopy, they proposed the following structure in the solid state with tin in a trigonal-bipyramidal environment:

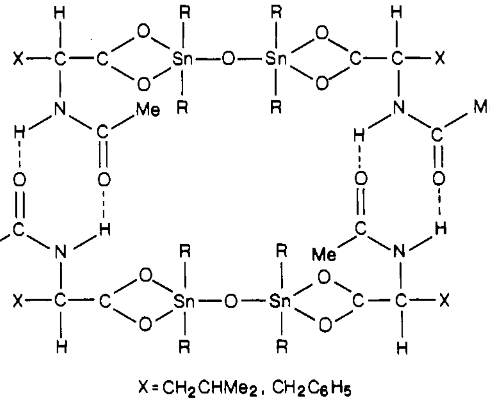

X = CH_2CHMe_2, $CH_2C_6H_5$

In this instance, linear R–Sn–R groups are suggested,[14] thus placing the R groups in axial positions, whereas the stannoxane compositions uniformly have been found[5,7-13] to possess equatorially situated R groups. In solution, dissociation of the tetranuclear complex into two stannoxane fragments is proposed[14] with rupture of the hydrogen-bonding network.

Studies with substituted carboxylic acids again reveal tetranuclear tin compositions containing diorganotin $[R_2XSnOSnR_2X']_2$ moieties e.g., $\{[(n\text{-}Bu)_2SnO_2CCCl_3]_2O\}_2$,[15] $[(Me_2SnO_2CCF_3)_2O]_2$,[16] and $[(Me_2SnO_2CCH_2Cl)_2O]_2$.[17] All of these oxodiorganotin carboxylates have been subjected to X-ray analysis and reveal planar structures containing the Sn_2O_2 unit, analogous to the "ladder" structures initially referred to.

Less is known about the structures of the corresponding "anhydrides", i.e., the diorganotin carboxylates. Interestingly, the dimethyltin chloracetate complex $[Me_2SnO_2CCH_2Cl]_2$[18] resulted from the solvolysis of hexamethyltin by monochloroacetic acid with cleavage of tin–carbon bonds in chloroform solution at 35 °C, according to (1). The crystal structure[18] showed two

$$Me_3SnSnMe_3 + 2ClCH_2CO_2H \xrightarrow{CHCl_3} [Me_2SnO_2CCH_2Cl]_2 + 2CH_4 \quad (1)$$

trigonal-bipyramidal tin centers linked equatorially by the Sn–Sn bond with internuclear bridging carboxylate groups spanning axial positions. The only example of a diorganotin dicarboxylate structural analysis is that recently reported for $Me_2Sn(O_2CCH_3)_2$.[19] It was found to consist of a distorted octahedral conformation.

We chose to study the formation of dimethyltin carboxylates by using anthranilic acid and its *p*-amino isomer. This afforded the possibility to investigate the influence of hydrogen bonding on structural preference as well as the competition of nitrogen and oxygen atoms for coordination to tin and, consequently, allowed us to compare our results with those of Sandhu et al.[14] We report the synthesis, solid-state X-ray characterization, and infrared and solution NMR behavior of $[(Me_2SnO_2CC_6H_4\text{-}o\text{-}NH_2)_2O]_2$ (**1**), $[(Me_2SnO_2CC_6H_4\text{-}p\text{-}NH_2)_2O]_2\cdot 4CH_3CN$, (**2**), and $Me_2Sn(O_2CC_6H_4\text{-}p\text{-}NH_2)_2$ (**3**). This choice of aminobenzoic acids has led us to the structural characterization of the first diorganotin dicarboxylate and its associated hydrolyzate. Also the synthesis and spectroscopic characterization of the cyclohexane carboxylate derivative $[(Me_2SnO_2CC_6H_{11})_2O]_2$ (**4**) is reported.

Experimental Section

The solvents used were of HPLC grade and were obtained from Fischer Scientific. Further purification of the solvents was done according to standard procedures.[20] Dimethyltin oxide (Pfaltz-Bauer) and the organic acids (Aldrich) were used as received. All synthetic operations were carried out in well-ventilated hoods.

^1H and ^{119}Sn NMR spectra were recorded on a Varian XL-300 FT NMR instrument operating at 300 and 111.862 HMz, respectively. Chemical shifts are reported with reference to TMS (^1H, internal standard) and tetramethyltin (^{119}Sn, external standard). Infrared spectra were recorded on a Perkin-Elmer Model 180 spectrometer using KBr windows. Spectra were recorded in Nujol.

Bis(μ_3-oxo)bis(μ-*o*-aminobenzoato-*O*,*O'*)bis(*o*-aminobenzoato)tetrakis[dimethyltin(IV)], $[(Me_2SnO_2CC_6H_4\text{-}o\text{-}NH_2)_2O]_2$ (1). To a suspension of dimethyltin oxide (1.16 g, 7.04 mmol) in benzene (200 mL) was added anthranilic acid (0.97 g, 7.07 mmol). The reaction mixture was heated under reflux for 3 h, with a Dean-Stark apparatus used for the azeotropic removal of water. After the reaction mixture was allowed to attain room temperature, ethanol (200 mL) was added and the reaction was continued for 4 h under reflux. A turbidity that was hitherto present in the solution disappeared, giving a clear solution. The reaction mixture was stirred at room temperature for 12 h. Removal of solvent yielded a solid. It was recrystallized from a mixture of methylene chloride and hexane (6:1) at room temperature: mp 241–243 °C dec (yield 1.9 g, 92%). ^1H NMR ($CDCl_3$/TMS; ppm): 7.82 (m), 7.30 (m), 6.71 (m), 5.7 (s, NH_2), 1.03 (Sn–CH_3 $^2J(^{119}Sn{-}C{-}^1H)$ = 87.0 Hz) 0.98 (Sn–CH_3, $^2J(^{119}Sn{-}C{-}^1H)$ = 85.0 Hz). ^{119}Sn NMR (DMSO; ppm): − 172.9, −190.5. IR (Nujol; cm^{-1}): 3460, 3320 (ν_{NH}); 1600, 1560 (ν_{COO}); 630 (ν_{SnO}). Anal. Calcd for $C_{36}H_{48}O_{10}N_4Sn_4$: C, 36.91; H, 4.13; N, 4.78. Found: C, 36.72; H, 4.07; N, 4.77.

Bis(μ_3-oxo)bis(μ-*p*-aminobenzoato-*O*,*O'*)bis(*p*-aminobenzoato)tetrakis[dimethyltin(IV)], $[(Me_2SnO_2CC_6H_4\text{-}p\text{-}NH_2)_2O]_2\cdot 4CH_3CN$ (2). Dimethyltin oxide (1.06 g, 6.43 mmol) and *p*-aminobenzoic acid (0.88 g,

---

(6) Pfeiffer, P.; Brach, O. *Z. Anorg. Chem.* **1914**, *87*, 229.
(7) Alleston, D. L.; Davies, A. G.; Hancock, M.; White, R. F. M. *J. Chem. Soc.* **1963**, 5469.
(8) Harrison, P. G.; Begley, M. J.; Molloy, K. C. *J. Organomet. Chem.* **1980**, *186*, 213.
(9) Puff, H.; Friedrichs, E.; Visel, F. *Z. Anorg. Allg. Chem.* **1981**, *477*, 50.
(10) Chow, Y. M. *Inorg. Chem.* **1971**, *10*, 673.
(11) Okawara, R. *Proc. Chem. Soc., London* **1961**, 383.
(12) Okawara, R.; Kasai, N.; Yasuda, K. *Second International Symposium on Organometallics Chemistry*; University of Wisconsin: Madison, WI, 1965; p 128.
(13) Puff, H.; Bung, I.; Friedrichs, E.; Jansen, A. *J. Organomet. Chem.* **1983**, *254*, 23.
(14) Sandhu, G. K.; Gupta, R.; Sandhu, S. S.; Parish, R. V. *Polyhedron* **1985**, *4*, 81.
(15) Graziani, R.; Bombieri, G.; Forsellini, E.; Furlan, P.; Peruzzo, V.; Tagliavini, G. *J. Organomet. Chem.* **1977**, *125*, 43.
(16) Faggiani, R.; Johnson, J. P.; Brown, I. D.; Birchall, T. *Acta Crystallogr., Sect. B: Struct. Crystallogr. Cryst. Chem.* **1978**, *B34*, 3743.
(17) Valle, G.; Peruzzo, V.; Tagliavini, G.; Ganis, P. *J. Organomet. Chem.* **1984**, *276*, 325.
(18) Faggiani, R.; Johnson, J. P. Brown, I. D.; Birchall, T. *Acta Crystallogr., Sect. B: Struct. Crystallogr. Cryst. Chem.* **1978**, *B34*, 3742.
(19) Lockhart, T. P.; Calabrese, J. C.; Davidson, F. *Organometallics* **1987**, *6*, 2479–2483.
(20) Vogel, A. I. *Textbook of Practical Organic Chemistry*; Longman: London, 1978.

6.42 mmol) were heated together in a mixture of benzene (200 mL) and ethanol (100 mL) for 4 h. The reaction mixture was filtered, and the solvent was removed to yield a solid. It was dissolved in a mixture of actonitrile, methylene chloride, and ethanol and kept for crystallization at room temperature. Large chunk-like crystals grew: mp 260–270 °C dec, sweats at 105 °C (yield 1.40 g, 74.3%). The crystals became opaque upon exposure to air, suggesting that they are losing solvent from the crystal lattice. ^{1}H NMR (DMSO-d_6/TMS; ppm): 7.64 (d) 6.56 (d) (aromatic), 5.8 (s, NH_2), 0.77 (s, Sn–CH_3), 0.69 (s, Sn–CH_3). ^{119}Sn NMR (DMSO-d_6/TMT; ppm): −208.4, −217.0. IR (Nujol; cm^{-1}): 3460 (ν_{NH}); 1590, 1550 (ν_{COO}); 600 (ν_{SnO}). Analysis was done on a sample that was pumped on in vacuum to remove solvent. Anal. Calcd for $C_{36}H_{48}O_{10}N_4Sn_4$: C, 36.91; H, 4.13; N, 4.78. Found: C, 36.78; H, 4.17; N, 4.70.

Bis(μ-*p*-aminobenzoato-*O*,*O*′)dimethyltin(IV), $Me_2Sn(O_2CC_6H_4$-*p*-$NH_2)_2$ (3). A mixture of dimethyltin oxide (1.28 g, 7.77 mmol) and *p*-aminobenzoic acid (2.13 g, 15.53 mmol) were taken in 250 mL of benzene and heated under reflux for 3 h in a Dean–Stark azeotropic distillation apparatus to remove the water formed in the reaction. A precipitate formed in the reaction. It was filtered, and the solvent was removed from the filtrate in vacuo to yield a slight amount of a precipitate. The two precipitates were dissolved in a minimum amount of hot acetonitrile (8 mL) and kept for crystallization in a refrigerator. The title compound grew in the form of pale brown crystals: mp 226 °C (yield 2.65 g, 81.0%). ^{1}H NMR ($CDCl_3$/TMS; ppm): 7.77 (d, 4 H), 6.65 (d, 4 H), 4.78 (s, 4 H, N*H*), 0.98 (s, 6 H, Sn–CH_3, $^2J(^{119}Sn–C–^1H)$ = 88.0 Hz). ^{119}Sn ($CDCl_3$; ppm): −226.2. Anal. Calcd for $C_{16}H_{18}O_4N_2Sn$: C, 45.65; H, 4.31; N, 6.65. Found: C, 45.68; H, 4.33; N, 6.69.

Bis(μ_3-oxo)bis(μ-cyclohexanoato-*O*,*O*′)bis(cyclohexanoato)tetrakis[dimethyltin(IV)], $[(Me_2SnO_2CC_6H_{11})_2O]_2$ (4). To a suspension of dimethyltin oxide (1.04 g, 6.31 mmol) in 200 mL of benzene was added cyclohexanecarboxylic acid (0.81 g, 6.32 mmol), and the mixture was heated under reflux for 2 h. A Dean–Stark apparatus was used for the azeotropic removal of water formed as a byproduct in the reaction. The reaction mixture was allowed to come to room temperature and filtered, and the solvent was removed in vacuo. The resulting solid was dissolved in methylene chloride (10 mL) and *n*-hexane (6 mL) and kept in the refrigerator for crystallization. After 2 days crystals suitable for X-ray analysis formed: mp 182–186 °C (yield 1.40 g, 78.2%). ^{1}H NMR ($CDCl_3$; ppm): centers of multiplets at 2.1, 1.8, 1.7, and 1.3; 0.85 (s), 0.83 (s); $^2J(^{119}Sn–C–^1H)$ = 85.0 and 83.0 Hz, respectively. ^{119}Sn NMR($CDCl_3$; ppm): −183.55, −189.72. IR (cm^{-1}): 1640, 1600, 1550 (ν_{COO}); 620 (ν_{SnO}). Anal. Calcd for $C_{36}H_{68}O_{10}Sn_4$: C, 38.07; H, 6.03. Found: C, 37.95; H, 5.99.

X-ray Studies. All X-ray crystallographic studies were performed on an Enraf-Nonius CAD4 diffractometer with graphite-monochromated molybdenum radiation ($\lambda(K\alpha_1)$ = 0.709 30 Å, $\lambda(K\alpha_2)$ = 0.713 59 Å) at an ambient temperature of 23 ± 2 °C. Details of the experimental and computational procedures have been described previously.[21]

Crystals were mounted in thin-walled glass capillary tubes, that were sealed as a precaution against moisture sensitivity. Data were collected using the θ–2θ scan mode for $2° \leq 2\theta_{Mo\,K\bar{\alpha}} \leq 43°$ for 1 and 2 and $2° \leq 2\theta_{Mo\,K\bar{\alpha}} \leq 50°$ for 3. The structures were solved by Patterson and difference Fourier techniques and were refined by full-matrix least-squares methods.[22]

X-ray Studies for $[(Me_2SnO_2CC_6H_4$-*o*-$NH_2)_2O]_2$ (1). Crystals of **1** are colorless laths that appear tan in bulk. The crystal used for the X-ray study was cut from a lath cluster and had approximate dimensions of 0.23 mm × 0.30 mm × 0.38 mm.

Crystal Data for 1. $[(Me_2SnO_2CC_6H_4$-*o*-$NH_2)_2O]_2$, triclinic space group $P\bar{1}$ [C_i^1-No. 2],[23] a = 8.792 (2) Å, b = 14.195 (2) Å, c = 18.324 (6) Å, α = 90.55 (2)°, β = 103.70 (2)°, γ = 93.87 (1)°, Z = 2, and $\mu_{Mo\,K\bar{\alpha}}$ = 2.296 mm^{-1}. A total of 5066 independent ($+h,\pm k,\pm l$) reflections were measured. No corrections were made for absorption.

The nitrogen atoms of the bridging *o*-aminobenzoate groups of the dimer containing Sn1 and Sn2 are disordered and were refined anisotropically as two independent atoms in half-occpancy (NA3 and NA7). Although the corresponding *o*-aminophenyl group in the second dimer was very poorly defined, only one position could be found for the nitrogen atom. Because of the poor definition, no attempt was made to refine the seven atoms of this group anisotropically. The remaining independent non-hydrogen atoms were refined anisotropically. Hydrogen atoms were omitted from the refinement. The final agreement factors[24] were R = 0.043 and R_w = 0.061 for the 4241 reflections having $I \geq 2\sigma_I$.

X-ray Studies for $[(Me_2SnO_2CC_6H_4$-*p*-$NH_2)_2O]_2 \cdot 4CH_3CN$ (2). Crystals of **2** are colorless laths that appear pale orange in bulk and degrade rapidly when removed from the mother liquor, presumably due to loss of acetonitrile of solvation. The crystal used for data collection (cut from a larger lath with approximate dimensions of 0.28 mm × 0.30 mm × 0.33 mm) showed no signs of degradation inside the sealed capillary tube.

Crystal Data for 2. $[(Me_2SnO_2CC_6H_4$-*p*-$NH_2)_2O]_2 \cdot 4CH_3CN$, monoclinic space group $P2_1/n$ (alternate setting of $P2_1/c$ [C_{2h}^5-No. 14][25]), a = 9.137 (1) Å, b = 11.867 (2) Å, c = 25.324 (3) Å, β = 91.48 (1)°, Z = 2 and $\mu_{Mo\,K\bar{\alpha}}$ = 1.867 mm^{-1}. A total of 3140 independent ($+h,+k,\pm l$) reflections were measured. No corrections were made for absorption.

The 30 independent non-hydrogen atoms comprising half of the dimer and one of the acetonitrile molecules were refined anisotropically. The three atoms of the second independent acetonitrile molecule were poorly defined and were refined isotropically. The eight independent aromatic hydrogen atoms were included in the refinement as fixed isotropic scatterers with calculated coordinates that were updated as refinement converged so that the final C–H bond lengths were 0.95 Å. The remaining hydrogen atoms were omitted from the refinement. The final agreement factors[24] were R = 0.043 and R_w = 0.060 for the 2610 reflections having $I \geq 2\sigma_I$.

X-ray Studies for $Me_2Sn(O_2CC_6H_4$-*p*-$NH_2)_2$ (3). Crystals of **3** are colorless laths that appear tan in bulk. The crystal used for the X-ray study had approximate dimensions of 0.25 mm × 0.30 mm × 0.38 mm.

Crystal Data for 3. $Me_2Sn(O_2CC_6H_4$-*p*-$NH_2)_2$, monoclinic space group $P2_1/n$,[25] a = 8.126 (3) Å, b = 19.810 (6) Å, c = 11.127 (3) Å, β = 99.09 (3)°, Z = 4, and $\mu_{Mo\,K\bar{\alpha}}$ = 1.475 mm^{-1}. A total of 3111 independent reflections ($+h,+k,\pm l$) were measured. No corrections were made for absorption.

The 23 independent nonhydrogen atoms were refined anisotropically. The eight independent aromatic hydrogen atoms were treated as described for **2**. The eight independent hydrogen atoms comprising the methyl groups and the nitrogen atom NA were located on a difference Fourier map and were included in the refinement as fixed isotropic scatterers. The hydrogen atoms on NB were omitted from the refinement. The final agreement factors[24] were R = 0.032 and R_w = 0.043 for the 2548 reflections having $I \geq 2\sigma_I$.

Results

The molecular geometry and atom-labeling scheme for the two unique molecules in **1** are shown in Figure 1. Atomic coordinates and selected bond lengths and angles are given in Tables I and II. The analogous information for **2** is given in Figure 2 and Tables III and IV and for **3** in Figure 3 and Tables V and VI. Thermal parameters, hydrogen atom parameters, and additional bond lengths and angles are provided as supplementary material.

Discussion

Synthesis. The oxo derivatives, **1**, **2**, and **4**, are formed in a condensation reaction between dimethyltin oxide and the respective carboxylic acid placed together in a 1:1 mole ratio in benzene or a benzene–ethanol solvent. Equation 2 illustrates the reaction

$$2Me_2SnO + 2(o\text{-}NH_2)C_6H_4CO_2H \rightarrow {}^1/_2[(Me_2SnO_2CC_6H_4\text{-}o\text{-}NH_2)_2O]_2 + H_2O \quad (2)$$

for **1**. Formation of the dimethyltin dicarboxylate **3**, followed the same reaction sequence, except a 1:2 mole ratio was used (eq 3).

$$Me_2SnO + 2(p\text{-}NH_2)C_6H_4CO_2H \rightarrow Me_2Sn(O_2CC_6H_4\text{-}p\text{-}NH_2)_2 + H_2O \quad (3)$$

The dicarboxylate, **3**, and the hydrolyzate, **2**, are related by the expression in (4). This process was indicated experimentally on

$$2[3] + H_2O \rightarrow {}^1/_2[2] + 2(p\text{-}NH_2)C_6H_4CO_2H \quad (4)$$

observation of the ^{119}Sn NMR pattern for a solution of **3**. In addition to the signal at −226.2 ppm, assigned to the one tin

---

(21) Sau, A.; C.; Day, R. O.; Holmes, R. R. *Inorg. Chem.* **1981**, *20*, 3076.

(22) The function minimized was $\sum w(|F_o| - |F_c|)^2$, where $w^{1/2} = 2F_o(Lp)/\sigma_I$. Mean atomic scattering factors were taken from ref 23; 1974; Vol. IV, pp 72–98. Real and imaginary dispersion corrections for Sn and O were taken from the same source, pp 149–150.

(23) *International Tables for X-ray Crystallography*; Kynoch: Birmingham, England, 1969; Vol. I, p 75.

(24) $R = \sum ||F_o| - |F_c|| / \sum |F_o|$ and $R_w = [\sum w(|F_o| - |F_c|)^2 / \sum w|F_o|^2]^{1/2}$.

(25) Reference 23; p 99.

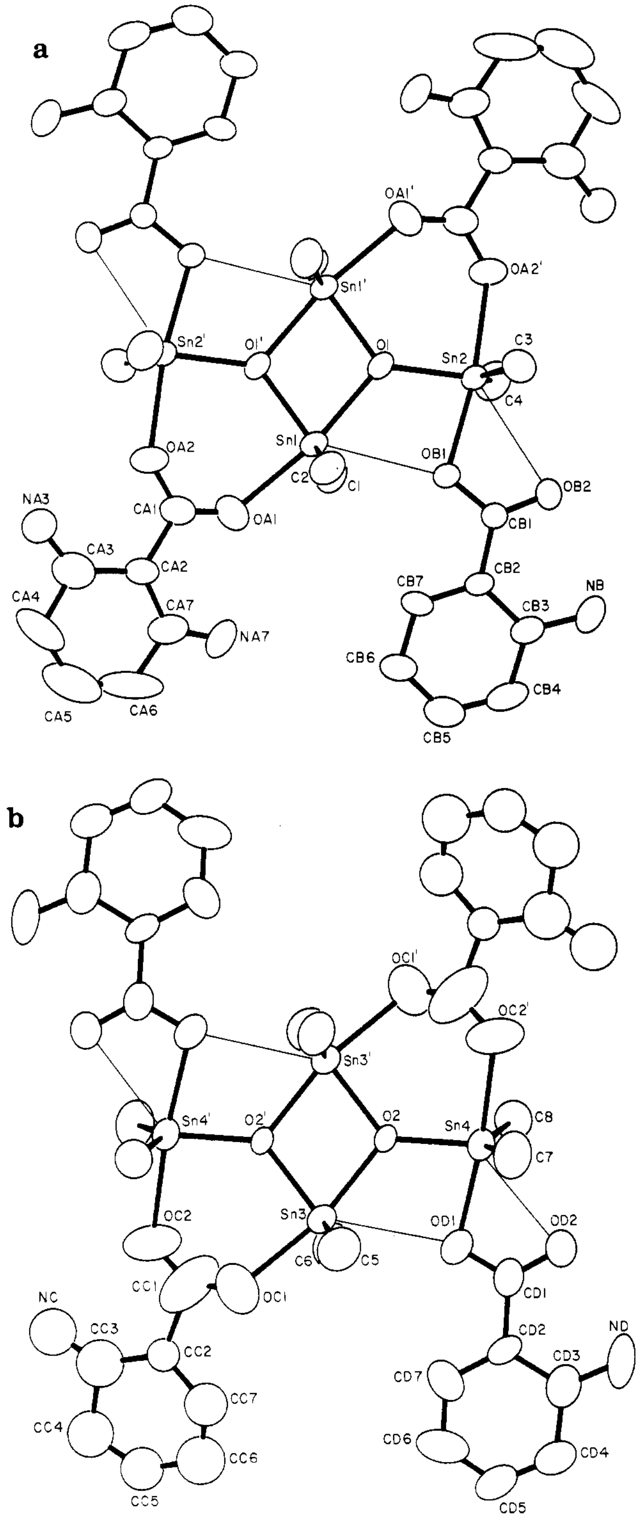

Figure 1. (a) ORTEP plot of one of the two independent molecules of $[(Me_2SnO_2CC_6H_4\text{-}o\text{-}NH_2)_2O]_2$ (**1**) with thermal ellipsoids at the 30% probability level. Weaker Sn–O interactions (2.877 (5), 2.909 (6) Å) are shown as narrow solid lines. Primed atoms are related to unprimed ones by $(-x, -y, -z)$. (b) ORTEP plot of the second of the two independent molecules of $[(Me_2SnO_2CC_6H_4\text{-}o\text{-}NH_2)_2O]_2$ (**1**) with thermal ellipsoids at the 30% probability level. Weaker Sn–O interactions (2.886 (7), 2.746 (7) Å) are shown as narrow solid lines. Primed atoms are related to unprimed ones by $(1 - x, 1 - y, 1 - z)$.

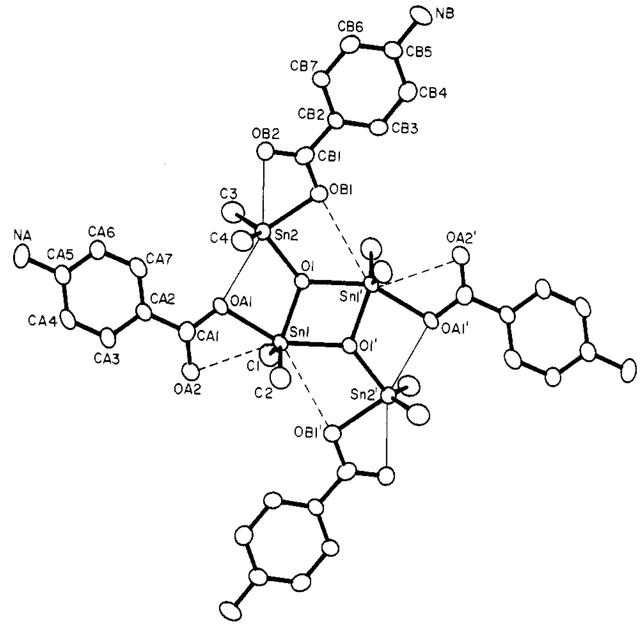

Figure 2. ORTEP plot of the $[(Me_2SnO_2CC_6H_4\text{-}p\text{-}NH_2)_2O]_2$ molecule (**2**) with thermal ellipsoids at the 30% probability level. Primed atoms are related to unprimed ones by $(-x, -y, -z)$. Intermediate Sn–O interactions (2.573 (6), 2.688 (5) Å) are shown as narrow solid lines. Long Sn–O interactions (2.935 (6), 3.315 (6) Å) are shown as dashed lines. Hydrogen atoms are omitted for purposes of clarity.

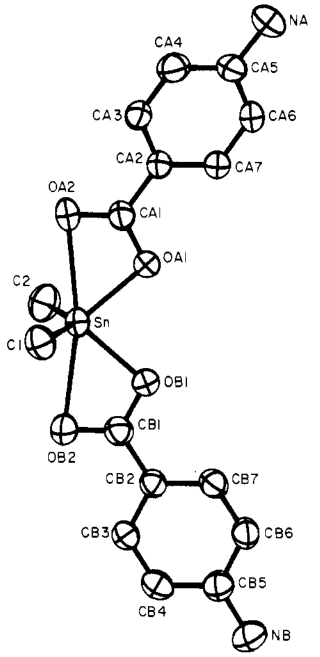

Figure 3. ORTEP plot of $Me_2Sn(O_2CC_6H_4\text{-}p\text{-}NH_2)_2$ (**3**) with thermal ellipsoids at the 50% probability level. Hydrogen atoms are omitted for purposes of clarity.

environment in **3**, two small peaks at −208.0 and −217.0 ppm were observed. These correspond to the hydrolysis product, **2**, as confirmed from its ^{119}Sn NMR spectrum.

The synthesis of the oxo compounds here contrasts with the formation of the trifluoroacetato derivative $[(Me_2SnO_2CCF_3)_2O]_2$, by Faggiani et al.,[16] which resulted when a chloroform solution of $[Me_2Sn(O_2CCF_3)]_2$ was heated. In this reaction (eq 5), rupture of the tin–tin bond occurred presumably in the presence of moisture.

$$2[Me_2SnO_2CCF_3]_2 + 2H_2O \xrightarrow{CHCl_3} [(Me_2SnO_2CCF_3)_2O]_2 + 2H_2 \quad (5)$$

Solid-State Structures. Oxo derivatives **1** and **2** have dimeric formulations where halves of the dimers are related by a crystallographic inversion center. For **1** there are two unique molecules that have nearly indistinguishable geometry. Both **1** and **2** have the same tin–oxygen "core" with two types of tin atoms: one type forms the central $(SnO)_2$ four-membered ring and the second type is pendant from the oxygen atoms of this ring, rendering them

Table I. Atomic Coordinates in Crystalline $[(Me_2SnO_2CC_6H_4\text{-}o\text{-}NH_2)_2O]_2$ (**1**)[a]

atom[b]	10^4x	10^4y	10^4z
Sn1	−961.0 (7)	853.7 (4)	252.4 (3)
Sn2	−1221.3 (7)	−1386.5 (4)	1208.0 (3)
Sn3	6524.1 (7)	5567.6 (4)	5578.5 (3)
Sn4	6635.4 (7)	2999.3 (5)	5415.9 (4)
O1	−505 (6)	−616 (4)	423 (3)
O2	5591 (6)	4199 (4)	5130 (3)
OA1	−1111 (12)	2393 (5)	−25 (5)
OA2	−269 (12)	2566 (6)	−1032 (5)
OB1	−2464 (7)	−145 (4)	1280 (3)
OB2	−3367 (8)	−943 (4)	2131 (4)
OC1	6908 (17)	7108 (8)	6003 (6)
OC2	5629 (12)	7971 (10)	5104 (7)
OD1	8521 (8)	4033 (5)	5997 (4)
OD2	9615 (9)	2701 (5)	6218 (5)
NA3	−433 (37)	4303 (17)	−1640 (13)
NA7	−2460 (32)	3832 (15)	441 (15)
NB	−5131 (12)	−102 (7)	2917 (5)
NC	6925 (35)	9950 (21)	5099 (18)
ND	12379 (14)	2687 (8)	7205 (8)
CA1	−937 (12)	2854 (8)	−550 (6)
CA2	−1510 (11)	3818 (7)	−611 (5)
CA3	−1178 (16)	4443 (10)	−1188 (7)
CA4	−1717 (21)	5368 (9)	−1224 (8)
CA5	−2445 (21)	5640 (11)	−717 (10)
CA6	−2729 (21)	5122 (13)	−201 (11)
CA7	−2285 (15)	4187 (9)	−134 (8)
CB1	−3298 (10)	−196 (6)	1791 (5)
CB2	−4066 (9)	652 (6)	1931 (4)
CB3	−4924 (11)	668 (7)	2489 (5)
CB4	−5643 (12)	1542 (9)	2575 (6)
CB5	−5480 (14)	2297 (7)	2130 (7)
CB6	−4675 (13)	2277 (7)	1587 (6)
CB7	−3953 (11)	1447 (6)	1508 (5)
CC1	6675 (25)	7756 (22)	5590 (10)
CC2	8049 (13)	8613 (8)	5853 (6)
CC3	7890 (24)	9539 (14)	5526 (17)
CC4	9411 (23)	10182 (14)	5816 (11)
CC5	10498 (19)	9736 (12)	6275 (10)
CC6	10600 (24)	8871 (15)	6596 (11)
CC7	9350 (20)	8388 (11)	6377 (9)
CD1	9636 (13)	3573 (8)	6333 (6)
CD2	10986 (10)	4115 (7)	6878 (5)
CD3	12286 (13)	3602 (8)	7261 (6)
CD4	13553 (12)	4188 (9)	7798 (6)
CD5	13436 (13)	5116 (10)	7855 (6)
CD6	12212 (18)	5566 (11)	7460 (8)
CD7	10986 (15)	5082 (8)	6975 (7)
C1	391 (13)	1363 (8)	1331 (6)
C2	−3255 (11)	586 (8)	−422 (5)
C3	−3170 (13)	−2305 (7)	682 (6)
C4	518 (12)	−1147 (9)	2231 (6)
C5	8185 (13)	5809 (9)	4935 (7)
C6	6231 (16)	5367 (10)	6682 (6)
C7	7509 (14)	2593 (9)	4480 (7)
C8	6089 (16)	2478 (10)	6416 (8)

[a] Numbers in parentheses are estimated standard deviations. [b] Atoms are labeled to agree with Figure 1.

tricoordinated. This six-atom core is nearly planar (±0.23 and ±0.06 Å for the two molecules for **1** and ±0.05 Å for **2**). The differences in the molecular geometries for **1** and **2** rest in the mode of bonding of the acid residue.

In molecules of **1**, two of the carboxylate ligands are pendant or anisobidentate while the remaining two form nearly symmetrical bridges between the two types of tin atoms. In **2** all of the carboxylate ligands are anisobidentate.

For **1**, the Sn–O bond lengths for the symmetrical bridges range from 2.254 (7) to 2.34 (1) Å. The pendant ligands have one normal ester linkage (Sn–O = 2.154 (5), 2.200 (7) Å) and two weaker interactions: one from the "acyl" oxygen atom to the same tin atom (2.909 (6), 2.746 (7) Å) and one from the ester oxygen atom to an adjacent tin atom (2.877 (5), 2.886 (7) Å). These longer values are considerably shorter than the van der Waals sum of 3.68 Å.[26]

Table II. Selected Bond Lengths (Å) and Angles (deg) in Crystalline $[(Me_2SnO_2CC_6H_4\text{-}o\text{-}NH_2)_2O]_2$ (**1**)[a]

Bond Lengths			
Sn1–O1	2.162 (6)	Sn3–O2	2.135 (6)
Sn1–C1	2.14 (1)	Sn3–C5	2.097 (9)
Sn1–C2	2.109 (9)	Sn3–C6	2.12 (1)
Sn1–OA1	2.254 (7)	Sn3–OC1	2.29 (1)
Sn1–O1′	2.029 (5)	Sn3–O2′	2.049 (5)
Sn2–O1	2.007 (5)	Sn4–O2	2.004 (5)
Sn2–C3	2.11 (1)	Sn4–C7	2.13 (1)
Sn2–C4	2.13 (1)	Sn4–C8	2.13 (1)
Sn2–OB1	2.154 (5)	Sn4–OD1	2.200 (7)
Sn2–OA2′	2.260 (7)	Sn4–OC2′	2.34 (1)
Sn1–OB1	2.877 (5)	Sn3–OD1	2.886 (7)
Sn2–OB2	2.909 (6)	Sn4–OD2	2.746 (7)
Bond Angles			
OA1–Sn1–O1	170.5 (3)	OC1–Sn3–O2	166.3 (4)
OA1–Sn1–C1	85.0 (4)	OC1–Sn3–C5	90.6 (5)
OA1–Sn1–C2	88.8 (4)	OC1–Sn3–C6	81.1 (5)
OA1–Sn1–O1′	94.2 (3)	OC1–Sn3–O2′	92.1 (4)
O1–Sn1–C1	96.2 (4)	O2–Sn3–C5	98.3 (4)
O1–Sn1–C2	95.5 (3)	O2–Sn3–C6	97.2 (4)
O1–Sn1–O1′	76.5 (2)	O2–Sn3–O2′	75.6 (2)
C1–Sn1–C2	144.6 (4)	C5–Sn3–C6	144.3 (5)
C1–Sn1–O1′	109.3 (3)	C5–Sn3–O2′	105.2 (4)
C2–Sn1–O1′	105.9 (3)	C6–Sn3–O2′	109.8 (4)
OA2′–Sn2–OB1	171.9 (3)	OC2′–Sn4–OD1	170.8 (4)
OA2′–Sn2–C3	86.2 (4)	OC2′–Sn4–C7	87.4 (5)
OA2′–Sn2–C4	83.6 (4)	OC2′–Sn4–C8	80.0 (5)
OA2′–Sn2–O1	91.2 (3)	OC2′–Sn4–O2	93.9 (4)
OB1–Sn2–C3	97.9 (3)	OD1–Sn4–C7	101.1 (4)
OB1–Sn2–C4	97.2 (4)	OD1–Sn4–C8	95.1 (4)
OB1–Sn2–O1	80.8 (2)	OD1–Sn4–O2	80.3 (2)
C3–Sn2–C4	142.4 (4)	C7–Sn4–C8	142.6 (5)
C3–Sn2–O1	109.1 (3)	C7–Sn4–O2	105.8 (4)
C4–Sn2–O1	107.2 (4)	C8–Sn4–O2	110.8 (4)

[a] Numbers in parentheses are estimated standard deviations. Atoms are labeled to agree with Figure 1.

Although there are two types of tin atoms in molecules of **1**, the geometry about these two types is essentially identical. To a first approximation the tin atoms are pentacoordinated and have trigonal-bipyramidal geometry, with the carbon atoms and a bridging oxygen atom occupying the equatorial plane. Each type of tin atom is, however, subjected to a sixth weaker interaction in the form of a carboxyl oxygen atom approaching one of the faces of the trigonal bipyramid (TBP). The affect of this sixth interaction can be seen in the angles between the three atoms defining this face. The axial–equatorial C–Sn–O angles are opened up relative to the 90° angle for the ideal TBP (values ranging from 95.1 (4) to 101.1 (4)°) while the equatorial C–Sn–C angle is considerably larger than the ideal value of 120° (values ranging from 142.4 (4) to 144.6 (4)°).

The molecular geometry for compound **2** differs from that of **1** in that the geometry about the two independent tin atoms is different. The entire molecule is nearly planar (±0.240 Å) with the exception of the methyl group atoms. As in the case of **1**, there are strong Sn–O bonds (2.009 (5)–2.206 (6) Å) as well as weaker Sn–O interactions (2.573 (6)–3.315 (6) Å).

When only the bonding interactions are considered, Sn1 is pentacoordinated with a distorted TBP geometry, where the atoms of the equatorial plane (Sn1, C1, C2, and O1) are coplanar to within ±0.031 Å. Alternatively, the geometry about Sn1 can be described as a bicapped trigonal bipyramid where the two capped faces (capped by atoms OA2 and OB1 at 2.935 (6) and 3.315 (6) Å from Sn1) share the edge defined by atoms C1 and C2. The angles about Sn1 involving the atoms defining the capped faces are all larger than those of the ideal TBP: The axial–equatorial angles range from 93.0 (3) to 97.4 (3)° while the equatorial–equatorial angle, C1–Sn1–C2, has a value of 137.2 (4)°. Concommitant with these distortions, the axial-axial angle, OA1–Sn1–O1′, is reduced to 151.2 (2)° with the oxygen atoms

---

[26] Bondi, A. *J. Phys. Chem.* **1964**, *68*, 441.

Table III. Atomic Coordinates in Crystalline $[(Me_2SnO_2CC_6H_4\text{-}p\text{-}NH_2)_2O]_2\cdot 4CH_3CN$ (**2**)[a]

atom[b]	10^4x	10^4y	10^4z
Sn1	1065.7 (6)	258.0 (5)	536.4 (2)
Sn2	−1904.8 (6)	2175.4 (5)	381.1 (2)
O1	−763 (6)	828 (5)	145 (2)
OA1	386 (6)	1685 (5)	1028 (2)
OA2	2398 (8)	1237 (6)	1498 (3)
OB1	−3258 (6)	1894 (5)	−291 (2)
OB2	−4075 (7)	3432 (6)	91 (3)
C1	547 (11)	−1017 (8)	1087 (4)
C2	2967 (10)	997 (9)	239 (4)
C3	−3189 (11)	1658 (10)	1020 (4)
C4	−599 (11)	3608 (8)	213 (4)
CA1	1300 (11)	1850 (8)	1430 (4)
CA2	985 (9)	2777 (7)	1802 (3)
CA3	1986 (11)	3055 (8)	2197 (4)
CA4	1701 (10)	3931 (9)	2539 (4)
CA5	409 (10)	4545 (8)	2501 (3)
CA6	−584 (10)	4244 (8)	2124 (4)
CA7	−310 (10)	3383 (9)	1772 (4)
NA	111 (10)	5437 (7)	2852 (3)
CB1	−4186 (10)	2741 (7)	−279 (4)
CB2	−5352 (9)	2794 (7)	−689 (3)
CB3	−5438 (10)	1996 (9)	−1081 (4)
CB4	−6591 (11)	2054 (8)	−1468 (4)
CB5	−7644 (10)	2896 (8)	−1449 (4)
CB6	−7527 (10)	3683 (8)	−1054 (4)
CB7	−6383 (10)	3641 (8)	−673 (4)
NB	−8763 (9)	2959 (7)	−1821 (3)
C5	1570 (15)	−682 (11)	4083 (5)
C6	2567 (16)	168 (12)	3903 (5)
N6	3342 (14)	874 (12)	3755 (5)
CN	−5109 (19)	5851 (16)	2240 (7)
C8	−4602 (20)	4738 (17)	2312 (7)
CN8	−4370 (18)	3770 (15)	2203 (17)

[a] Numbers in parentheses are estimated standard deviations. [b] Atoms are labeled to agree with Figure 2.

Table IV. Selected Bond Lengths (Å) and Angles (deg) in Crystalline $[(Me_2SnO_2CC_6H_4\text{-}p\text{-}NH_2)_2O]_2\cdot 4CH_3CN$ (**2**)[a]

	Bond Lengths		
Sn1–O1′	2.166 (5)	Sn2–O1	2.009 (5)
Sn1–O1	2.036 (5)	Sn2–OB1	2.104 (6)
Sn1–OA1	2.202 (6)	Sn2–OB2	2.573 (6)
Sn1–C1	2.119 (9)	Sn2–C3	2.114 (9)
Sn1–C2	2.103 (9)	Sn2–C4	2.126 (9)
Sn1–OA2	2.935 (6)	Sn2–OA1	2.688 (5)
Sn1–OB1′	3.315 (6)		
	Bond Angles		
OA1–Sn1–O1′	151.2 (2)	O1–Sn2–OB1	86.1 (2)
OA1–Sn1–C1	96.1 (3)	O1–Sn2–OB2	141.1 (2)
OA1–Sn1–C2	97.4 (3)	C3–Sn2–OA1	84.8 (3)
OA1–Sn1–O1	77.3 (2)	C3–Sn2–C4	135.3 (4)
C1–Sn1–C2	137.2 (4)	C3–Sn2–OB1	104.3 (3)
C1–Sn1–O1	111.2 (3)	C3–Sn2–OB2	87.0 (3)
O1′–Sn1–C1	94.2 (3)	OA1–Sn2–C4	82.1 (3)
O1′–Sn1–C2	93.0 (3)	OA1–Sn2–OB1	153.0 (2)
O1′–Sn1–O1	74.0 (2)	OA1–Sn2–OB2	151.0 (2)
C2–Sn1–O1	111.3 (3)	C4–Sn2–OB1	106.6 (3)
O1–Sn2–C3	107.4 (3)	C4–Sn2–OB2	84.9 (3)
O1–Sn2–OA1	66.9 (2)	OB1–Sn2–OB2	55.1 (2)
O1–Sn2–C4	82.1 (3)		

[a] Numbers in parentheses are estimated standard deviations. Atoms are labeled to agree with Figure 2.

Table V. Atomic Coordinates in Crystalline $Me_2Sn(O_2CC_6H_4\text{-}p\text{-}NH_2)_2$ (**3**)[a]

atom[b]	10^4x	10^4y	10^4z
Sn	3659.9 (3)	532.8 (1)	1654.5 (2)
OA1	6175 (3)	291 (2)	2041 (3)
OA2	4911 (4)	−364 (2)	3184 (3)
OB1	4501 (3)	1137 (1)	329 (3)
OB2	1849 (4)	1363 (2)	290 (3)
CA1	6237 (5)	−177 (2)	2861 (4)
CA2	7873 (5)	−462 (2)	3342 (4)
CA3	8018 (5)	−1060 (2)	3995 (4)
CA4	9551 (6)	−1330 (2)	4439 (4)
CA5	11010 (6)	−996 (3)	4253 (4)
CA6	10857 (6)	−387 (3)	3632 (5)
CA7	9328 (5)	−123 (3)	3165 (4)
CB1	3165 (5)	1468 (2)	−142 (4)
CB2	3270 (5)	1932 (2)	−1136 (4)
CB3	1873 (5)	2305 (2)	−1638 (4)
CB4	1965 (6)	2755 (3)	−2555 (4)
CB5	3447 (5)	2858 (2)	−3031 (4)
CB6	4833 (5)	2471 (2)	−2533 (4)
CB7	4747 (5)	2019 (2)	−1608 (4)
C1	2322 (6)	−251 (2)	685 (4)
C2	3259 (6)	1162 (3)	3097 (4)
NA	12571 (5)	−1254 (3)	4680 (5)
NB	3500 (6)	3376 (2)	−3961 (4)

[a] Numbers in parentheses are estimated standard deviations. [b] Atoms are labeled to agree with Figure 3.

Table VI. Selected Bond Lengths (Å) and Angles (deg) in Crystalline $Me_2Sn(O_2CC_6H_4\text{-}p\text{-}NH_2)_2$ (**3**)[a]

	Bond Lengths		
Sn–C1	2.094 (5)	Sn–OB2	2.543 (3)
Sn–C2	2.099 (5)	OA1–CA1	1.296 (5)
Sn–OA1	2.077 (3)	OA2–CA1	1.244 (8)
Sn–OA2	2.556 (3)	OB1–CB1	1.305 (5)
Sn–OB1	2.097 (3)	OB2–CB1	1.258 (5)
	Bond Angles		
C1–Sn–C2	134.7 (2)	OA1–Sn–OB1	81.8 (1)
C1–Sn–OA1	110.5 (2)	OA1–Sn–OB2	136.9 (1)
C1–Sn–OA2	87.0 (2)	OA2–Sn–OB1	136.5 (1)
C1–Sn–OB1	105.2 (2)	OA2–Sn–OB2	168.0 (1)
C1–Sn–OB2	88.1 (2)	OB1–Sn–OB2	55.5 (1)
C2–Sn–OA1	104.2 (2)	Sn–OA1–CA1	103.8 (2)
C2–Sn–OA2	89.8 (2)	Sn–OA2–CA1	82.7 (3)
C2–Sn–OB1	107.8 (2)	Sn–OB1–CB1	103.1 (2)
C2–Sn–OB2	85.8 (2)	Sn–OB2–CB1	83.6 (2)
OA1–Sn–OA2	55.0 (1)		

[a] Numbers in parentheses are estimated standard deviations. Atoms are labeled to agree with Figure 3.

bent away from the capping atoms.

The geometry about Sn2 for compound **2** is very similar to the geometry found for the diorganotin dicarboxylate monomer, **3** (vide infra). This geometry is best described as a bicapped tetrahedron, where the capping atoms OB2 and OA1 are at respective distances of 2.573 (6) and 2.688 (5) Å from Sn2. The angle OB2–Sn2–OA1 has a value of 151.0 (2)° and the atoms Sn2, OB2, OA1, and O1 are coplanar to within ±0.054 Å. The four atoms comprising the tetrahedron (OB1, O1, C3, and C4) have four "normal" tetrahedral angles about Sn2 (104.3 (3)–107.4 (3)°) and two angles that show the effects of the capping atoms (OB1–Sn2–O1 = 86.1 (2)°, C3–Sn2–O4 = 135.3 (4)°).

The interconversion of the molecular geometry for **2** into the molecular geometry for **1** can be easily visualized. All that is required is a 180° rotation of two aminobenzoate units about the Sn1–OA1 and Sn1–OA1′ bonds and the formation of two bonds between OA2 and Sn2 and between OA2′ and Sn2′.

The molecular geometry about the Sn atom in **3** is best described as a bicapped tetrahedron as was described for Sn2 in **2**. The atoms forming the tetrahedron (C1, C2, OA1, and OB1) form four "normal" tetrahedral angles about the Sn atom (104.2 (2)–110.5 (2)°) and form two angles that show the effect of the capping atoms (OA1–Sn–OB1 = 81.8 (1)°, C1–Sn–C2 = 134.7 (2)°). The capping atoms OA2 and OB2 are at respective distances of 2.556 (3) and 2.543 (3) Å from the tin atom. The atoms Sn, OA2, OB2, OA1, and OB1 are coplanar to within ±0.094 Å.

Although the majority of the amino group hydrogen atoms could not be located, there are intermolecular N–O distances in **2** and **3** that suggest hydrogen-bonding interactions. Specifically, for **2** intermolecular distances between NA and OA2 have a value of 2.93 (1) Å, while for **3** the intermolecular distances NB–OB2 and NA–OA2 have values of 3.041 (6) Å and 3.241 (6) Å, respectively. For **1**, the molecular geometry suggests intramolecular hydrogen bonding between the hydrogen atoms of the *o*-amino groups and the adjacent carboxylate oxygen atoms. We had established this feature previously in the triphenyltin ester of anthranilic acid, $Ph_3Sn(O_2CC_6H_4\text{-}o\text{-}NH_2)$.[27]

Structural Comparisons. The diorganooxotin carboxylates cited previously, $\{[(n\text{-Bu})_2SnO_2CCCl_3]_2O\}_2$,[15] $[(Me_2SnO_2CCF_3)_2O]_2$,[16] and $[(Me_2SnO_2CCH_2Cl)_2O]_2$,[17] all have solid-state structures closely resembling the anthranilic acid derivative, **1**, both in the immediate geometry around each type of tin atom and in the presence of two different types of coordination of the carboxylate groups; i.e., each of these derivatives has one pair of pendant carboxylate ligands and one pair that behaves in a bidentate fashion and span the two types of tin atoms. The isolation of the p-aminobenzoate isomer, **2**, as a lone example containing all pendant carboxylate ligands, Figure 2, may be influenced by the added stability that could result from intermolecular hydrogen bonding uniquely provided by the *p*-amino groups and the two carboxylate units attached to Sn1 and Sn1′. In the anthranilic acid derivative, **1**, the *o*-amino groups are positioned for intramolecular hydrogen bonding within each carboxylate unit.

The similarity between the structures of **1**–**3** and the previous literature examples cited extends to a comparison of the ranges of Sn–O carboxylate bond lengths that are considered strong bonds and those that are classified as weak interactions. The former Sn–O bond lengths for **1**–**3** lie in the range 2.1–2.3 Å (2.2–2.4 Å for the literature examples). The weaker Sn–O bond lengths cover the range 2.5–2.9 Å for **1**–**3** and 2.7–3.1 Å for the literature examples.

Previous infrared and vapor-phase molecular weight measurements indicated that the solid-state structure of $\{[(n\text{-Bu})_2SnO_2CCCl_3]_2O\}_2$ was retained in solution.[15] Two asymmetric carbonyl absorptions are present in the solid and in CCl_4 solution where a molecular weight corresponding to the latter formulation is obtained. One band at 1685 cm^{-1} is ascribed to the monodentate chloroacetate group. The other band at 1650 cm^{-1} is assigned to stretching of the bidentate carboxylate group. We observed similar carbonyl absorptions in the solid state for **1**, **2**, and **4**. More to the point, our solution-state ^{119}Sn NMR measurements show two resonances for **1**, **2**, and **4** and one resonance for **3** in keeping with the X-ray structures established for **1**–**3**. The cyclohexanoato derivative, **4**, is expected to have a structure analogous to that found for **1** and **2**.

Sandu et al.[14] prepared 1:1 and 2:1 *N*-acetylamino acid complexes by reacting the amino acids with dialkyltin oxide in a benzene–ethanol mixture analogous to the synthetic procedures reported here. The formulation of the 1:1 complexes proposed for the solid state, $[(R_2LSn)_2O]_2$, is the same as that reported here for **1** and **2** from X-ray studies. However, as depicted in the introduction, Sandhu et al.[14] suggest an entirely different structural arrangement showing axial alkyl groups in a trigonal-bipyramidal geometry. Equivalent tin atoms are indicated with dimeric units held together by hydrogen bonding. The 2:1 complexes are proposed[14] to have dimeric solid-state structures, $[R_2SnL_2]_2$, in contrast to the monomeric structure observed for **3** having this empirical composition. In view of our results showing that hydrogen bonding from amino groups, whether inter- or intramolecular, appears to have little effect on the ultimate structure obtained and that there is a close structural correspondence of the aminobenzoic acid derivatives, **1**–**3**, with previous literature[15–17] on related diorganotin carboxylates that contain no hydrogen-bonding features, it is probable that the *N*-acetylamino acid derivatives[15] also possess structures similar to the ones reported in the present investigation.

Acknowledgment. The support of this research by the National Science Foundation (Grant CHE-8504737) and the donors of the Petroleum Research Fund, administered by the American Chemical Society, is gratefully acknowledged. We also thank the University of Massachusetts Computing Center for generous allocation of computer time.

Registry No. **1**, 112219-86-0; **2**, 112246-97-6; **3** (coordination compound entry), 112219-87-1; **3** (stannane entry), 112219-89-3; **4**, 112219-88-2; ^{119}Sn, 14314-35-3; anthranilic acid, 118-92-3; *p*-aminobenzoic acid, 150-13-0; cyclohexanecarboxylic acid, 98-89-5; dimethyltin oxide, 2273-45-2.

Supplementary Material Available: Listings of thermal parameters and additional bond lengths and angles for **1** (Tables S1 and S2) and thermal parameters, hydrogen atom parameters, and additional bond lengths and angles for **2** and **3** (Tables S3–S5 and S6–S8, respectively) (8 pages); tables of observed and calculated structure factor amplitudes for **1**–**3** (36 pages). Ordering information is given on any current masthead page.

---

[27] Swisher, R. G.; Vollano, J. F.; Chandrasekhar, V.; Day, R. O.; Holmes, R. R. *Inorg. Chem.* **1984**, *23*, 3147.

Additions and Corrections

1987, Volume 26

Sanat K. Mandal, Laurence K. Thompson,* Eric J. Gabe, Florence L. Lee, and Jean-Pierre Charland: Spontaneous Reduction of Copper(II) Complexes of the Ligand 3,6-Bis(2-pyridylthio)pyridazine. Crystal Structures of Bis[3,6-bis(2-pyridylthio)pyridazine-N^1,N^2]aquocopper(II) Diperchlorate Trihydrate and Bis[μ-3,6-bis(2-pyridylthio)pyridazine-N^4,μ-N^1,μ-N^2,N^3]dicopper(I) Diperchlorate.

Page 2385. Atomic positional parameters (Table II) should read as follows: Cu, $x = 0.50000$ (0), $z = 0.25000$ (0); N(2), $y = 0.2243$ (7).—Laurence K. Thompson